OPEN

Initial Experience Using ^{99m}Tc-MIBI SPECT/CT for the Differentiation of Oncocytoma From Renal Cell Carcinoma

Steven P. Rowe, MD, PhD, Michael A. Gorin, MD,† Jennifer Gordetsky, MD,‡ Mark W. Ball, MD,† Phillip M. Pierorazio, MD,† Takahiro Higuchi, MD, PhD,§ Jonathan I. Epstein, MD,‡ Mohamad E. Allaf, MD,† and Mehrbod S. Javadi, MD**

Purpose: The differentiation of oncocytoma from renal cell carcinoma (RCC) remains a challenge with currently available cross-sectional imaging techniques. As a result, a large number of patients harboring a benign oncocytoma undergo unnecessary surgical resection. In this study, we explored the utility of ^{99m}Tc-MIBI SPECT/CT for the differentiation of these tumors based on the hypothesis that the large number of mitochondria in oncocytomas would lead to increased ^{99m}Tc-MIBI uptake.

Patients and Methods: In total, 6 patients (3 with oncocytoma and 3 with RCC) were imaged with ^{99m}Tc-MIBI SPECT/CT. Relative quantification was performed by measuring tumor-to-normal renal parenchyma background ratios.

Results: All 3 oncocytomas demonstrated radiotracer uptake near or above the normal renal parenchymal uptake (range of uptake ratios, 0.85–1.78). In contrast, the 3 RCCs were profoundly photopenic relative to renal background (range of uptake ratios, 0.21–0.31).

Conclusions: ^{99m}Tc-MIBI SPECT/CT appears to be of value in scintigraphically distinguishing benign renal oncocytoma from RCC.

Key Words: oncocytoma, renal cell carcinoma, ^{99m}Tc-MIBI, SPECT/CT

(*Clin Nucl Med* 2015;40: 309–313)

Because of the growing use of cross-sectional imaging, the incidence of asymptomatic small renal tumors has risen steadily over the last several decades.[1,2] Although most of these lesions represent renal cell carcinoma (RCC), up to 20% will be one of several benign histologies including oncocytoma, angiomyolipoma, metanephric adenoma, and mixed epithelial stromal tumor.[3] Among these lesions, oncocytoma is the most common, accounting for up to 15% of all renal tumors. Unfortunately, conventionally utilized imaging modalities are unable to reliably differentiate oncocytoma from RCC.[4,5] As a result, many patients harboring an oncocytoma needlessly proceed to surgical resection. A recent estimate suggests that more than 5600 benign renal masses are resected yearly in the United States.[6]

Compared with other renal masses, oncocytomas are unique in that at the ultrastructural level, these tumors are composed of cells with numerous densely packed mitochondria.[7,8] Taking advantage of this property, Gormley and coworkers[9] tested whether oncocytomas could be differentiated from other renal tumors using the mitochondrial imaging agent ^{99m}Tc-MIBI. To this end, the authors studied 6 patients with renal tumors (1 oncocytoma, 1 angiomyolipoma, 1 simple cyst, and 3 RCCs) using planar ^{99m}Tc-MIBI imaging.[9] Compared with the adjacent normal renal parenchyma, the 1 oncocytoma showed a 1.44-fold increase in MIBI uptake. In contrast, the 5 other lesions appeared photopenic (range of uptake ratios, 0.55–0.86). Although this latter finding is consistent with the handful of other studies that have described RCCs as poorly avid for ^{99m}Tc-MIBI,[10–13] this remains the only known report of an oncocytoma imaged with ^{99m}Tc-MIBI.

Combined, the previously cited data provide strong preliminary support for the use of ^{99m}Tc-MIBI imaging to aid in the differentiation of oncocytomas from other renal masses. Herein we expand on the existing literature by reporting our initial experience imaging renal tumors, including 3 biopsy-proven oncocytomas, using ^{99m}Tc-MIBI SPECT/CT.

PATIENTS AND METHODS

Study Cohort

After institutional review board approval, 3 patients with a history of oncocytoma on previous percutaneous needle biopsy were consented to undergo ^{99m}Tc-MIBI SPECT/CT imaging. In addition, 3 patients with unknown renal masses who elected surgical resection were consented to undergo imaging within 1 week before surgery. Both biopsy and resection specimens were centrally reviewed by 2 pathologists with expertise in genitourinary pathology. Notably, the 3 patients who underwent surgical resection were found to have RCC on final pathology. Table 1 provides details of the study cohort.

Imaging Protocol

Patients were kept nil per os for approximately 6 hours and then intravenously administered 925 MBq (25 mCi) of ^{99m}Tc-MIBI. Immediately after radiotracer injection, 30 dynamic 1-minute planar frames were acquired with a 64 × 64 pixel matrix size using a Siemens Symbia 16-slice SPECT/CT (Erlangen, Germany) system with low-energy high-resolution collimators. This dynamic phase was then followed by a 28-minute SPECT/CT acquisition. SPECT imaging was acquired initially in step and shoot mode at 28 seconds per step with 60 steps. Detector range was set to 180 degrees per detector. CT images were acquired at 130 kV and 90 mA with dose care modulation enabled. The 3-mm axial images were reconstructed for both SPECT and CT data sets. The first patient demonstrated high renal parenchymal background uptake after directly starting SPECT/CT acquisition post planar imaging. As such, it was postulated that a delayed SPECT acquisition would potentially be of value. Hence, an additional 17-minute SPECT was acquired immediately after the first SPECT (step and shoot mode at 17 seconds per step with 60 steps and 180 degree detector range), and the relative tumor-to-background ratio appeared to visually improve. For the sake of consistency and visual diagnostic accuracy, all future patients underwent 30 minutes of planar dynamic imaging directly after injection followed by a 17-minute SPECT/CT at 75 minutes after injection (Fig. 1). The length of the 45-minute delay between the dynamic and SPECT acquisitions was chosen as a compromise between maximizing tumor-to-background ratio and still maintaining a reasonable workflow and overall study time.

Received for publication October 31, 2014; revision accepted November 12, 2014.

From the *The Russell H. Morgan Department of Radiology and Radiological Science, †The James Buchanan Brady Urological Institute and Department of Urology, and ‡Department of Pathology, Johns Hopkins University School of Medicine, Baltimore, MD; and §Department of Nuclear Medicine, University of Würzburg, Würzburg, Germany.

Conflicts of interest and sources of funding: Supported by the Buerger Family Scholar Fund and a grant from the National Kidney Foundation of Maryland.

Reprints: Mehrbod S. Javadi, MD, Johns Hopkins Bayview Medical Center, 4940 Eastern Ave, Baltimore, MD 21224. E-mail: mjavadi@jhmi.edu.

ISSN: 0363-9762/15/4004–0309

TABLE 1. Study Cohort Characteristics

Patient Number	Sex	Age	Tumor Diameter on Imaging, cm	Pathology	Relative Uptake
1	Male	69	6.2	Oncocytoma	1.78
2	Male	78	2.5	Oncocytoma	0.85
3	Male	78	4.6	Oncocytoma	1.10
4	Male	45	5.5	Clear cell RCC, grade III	0.26
5	Male	38	2.8	Unclassified RCC	0.21
6	Female	48	3.1	Xp11 Translocation RCC	0.31

Image Analysis

SPECT and CT images were exported to a Mirada Medical workstation (Oxford, United Kingdom). Manual rigid registration with the Mirada software was used to optimally register the SPECT and CT images. The images were reviewed by 2 readers with expertise in nuclear medicine imaging and consensus as to the location of the mass, and the highest uptake site within the mass and the ipsilateral normal renal parenchyma was reached. Renal parenchymal uptake was determined by manual placement spherical volume of interest within the consensus highest uptake portion of the normal parenchyma on the attenuation corrected SPECT images. Tumor uptake was similarly determined through an analogous placement of a spherical volume of interest within the highest uptake portion of the tumor, again using the attenuation corrected SPECT images. Maximum uptake values were recorded for the normal parenchyma and tumors. Relative tumor uptake values were calculated from the ratios of maximum tumor uptake to maximum normal renal parenchymal uptake.

RESULTS

Dynamic Planar Imaging

The dynamic planar images of the 3 patients with known oncocytomas were qualitatively reviewed. The 2 larger oncocytomas demonstrated relative photopenia in the locations of the tumors on early dynamic images with gradual fill-in to approximately the uptake level of the background renal parenchyma or higher at the end of the dynamic phase (Fig. 2). The smallest oncocytoma imaged (patient 2) was difficult to resolve on the dynamic planar images, emphasizing the importance of the subsequent SPECT acquisition. The planar images for the patients with RCC were also reviewed, and for those masses large enough to resolve on the planar imaging, the early appearance was similar to that for oncocytoma with relative photopenia. However, later fill-in with radiotracer was not visually observed (data not shown). A final observation from the dynamic planar images is that a fraction of the injected ^{99m}Tc-MIBI quickly washes through the kidneys and is excreted into the urine, whereas the majority of the radiotracer that reaches the kidneys accumulates in the renal parenchyma and is not washed out. Indeed, at the end of 30 minutes of dynamic images, there was no qualitative evidence of radiotracer within the renal collecting systems. These observations have previously been suggested in work that evaluated the utility of ^{99m}Tc-MIBI as a renal functional imaging agent.[14]

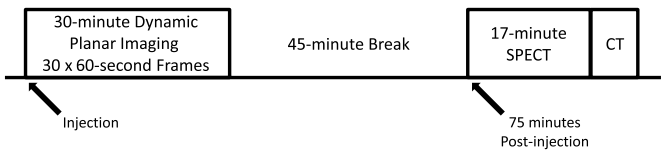

FIGURE 1. Line-block diagram of the imaging protocol used to obtain the planar, SPECT, and SPECT/CT images.

SPECT/CT Imaging

The 3 known oncocytomas demonstrated maximum radiotracer uptake similar to or above uptake levels within the adjacent renal parenchyma (average tumor uptake, 1.19; range, 0.85–1.78; Table 1; Fig. 3). In 2 of the patients with oncocytomas, prominent hypoenhancing central scars were observed on separate contrast-enhanced CT scans, and these were also well appreciated as prominent central photopenic defects on ^{99m}Tc-MIBI SPECT/CT (patients 1 and 3, Fig. 3). In contrast to the oncocytomas, the 3 RCCs were markedly photopenic relative to the background renal parenchyma, with an average tumor uptake of 0.26 (range, 0.21–0.31; Table 1; Fig. 4). This equates to a greater than 4-fold increase in relative uptake between oncocytoma and RCC, further reinforcing the utility of qualitative assessment of tumor uptake differences.

DISCUSSION

The results of this study highlight a potential role for ^{99m}Tc-MIBI SPECT/CT in the evaluation of renal masses. In this small series of patients, all pathologically proven oncocytomas demonstrated significant ^{99m}Tc-MIBI uptake near or above that of the background normal renal parenchyma, whereas the pathologically proven RCCs were markedly photopenic. Although this small pilot study is not powered to detect a statistically significant difference between the relative uptake values of the oncocytomas and the RCCs, our observations seem to indicate a profound difference in the ^{99m}Tc-MIBI uptake behavior of these 2 types of renal masses. The total uptake difference between the oncocytomas and RCCs was large enough that visual analysis could

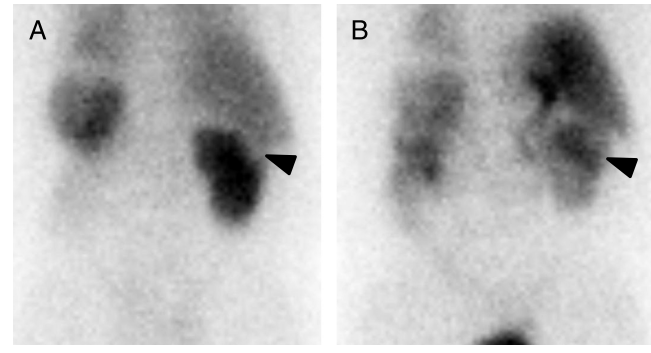

FIGURE 2. A, One-minute postinjection posterior dynamic planar image of patient 1 demonstrating a subtle photopenic defect in the cortex of the upper pole of the right kidney at the site of the patient's known oncocytoma (arrowhead). The patient was status post-left nephrectomy, hence the lack of visualization of the left kidney. **B**, Thirty-minute postinjection posterior dynamic planar image of the same patient. There has been fill-in of the large right upper pole oncocytoma (arrowhead) with relative retention of radiotracer in the mass higher than that in the surrounding normal renal parenchyma.

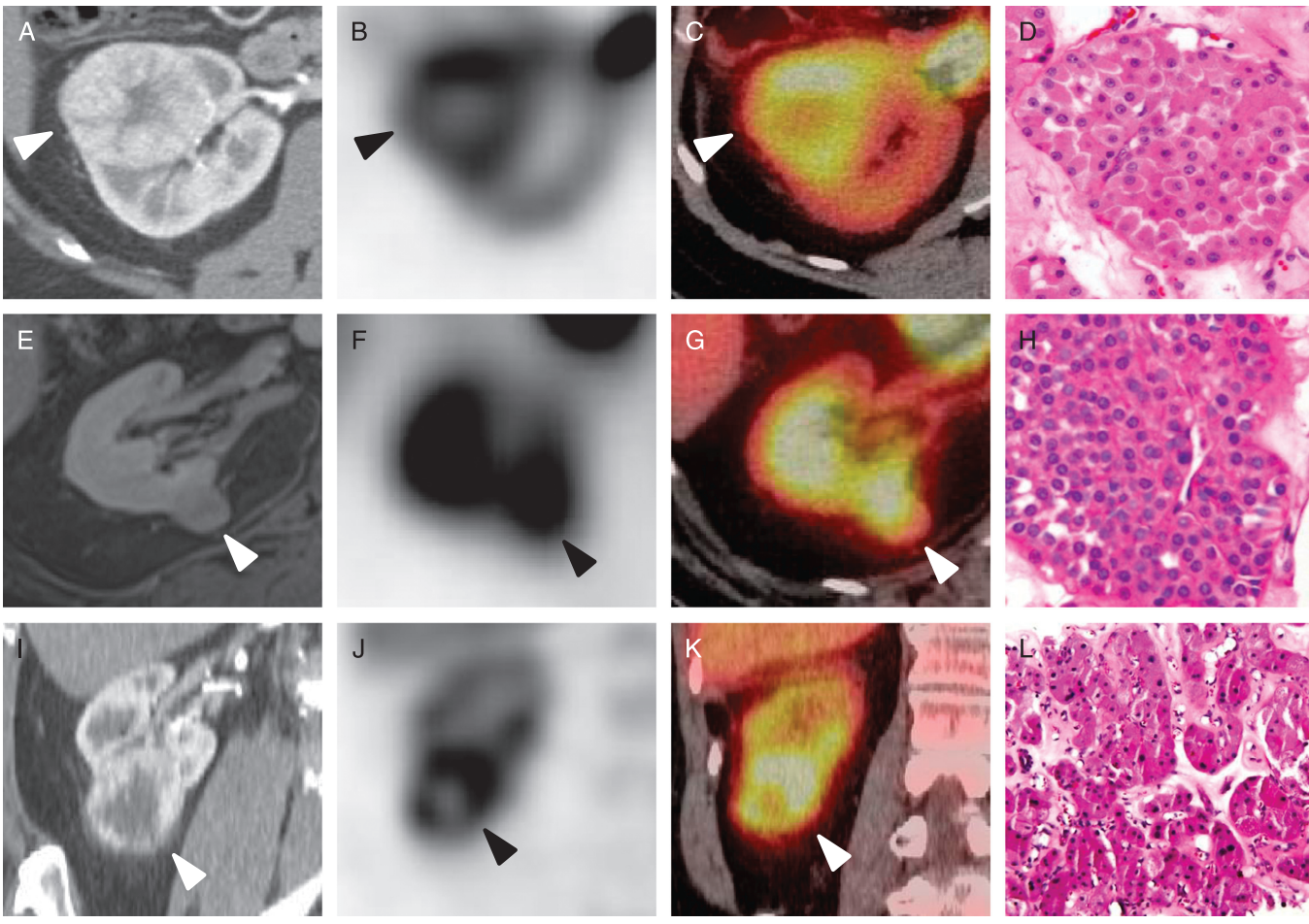

FIGURE 3. Representative images of the oncocytomas included in this study. **A**, Axial contrast-enhanced CT, axial SPECT (**B**), and axial SPECT/CT fusion images of a right upper pole oncocytoma (**C**) with a representative histologic image (**D**, hematoxylin and eosin stain [HE] ×20) (patient 1, white and black arrowheads). **E**, Axial contrast-enhanced T1-weighted MRI, axial SPECT (**F**), and axial SPECT/CT fusion images of a right medial interpolar oncocytoma (**G**) with an accompanying histologic image (**H**, HE ×20) (patient 2, white and black arrowheads). I, Coronal contrast-enhanced CT, coronal SPECT (**J**), and coronal SPECT/CT fusion images of a right lower pole oncocytoma (**K**) with a corresponding histologic image (**L**, HE ×20) (patient 3, white and black arrowheads).

reliably differentiate the lesions (Figs. 3, 4) without having to rely on relative quantitative assessment.

Among the imaged oncocytomas, there was a relatively wide range of uptake values relative to the normal renal parenchyma. The reason for these uptake differences among tumors of the same histologic type is not immediately apparent. Interestingly, the oncocytoma with the most elevated uptake (patient 1) was also the largest tumor imaged and was 1 of the 2 tumors with a prominent central scar on contrast-enhanced CT and the SPECT portion of our study. Whether some aspect of an oncocytoma that would cause it to grow to a large size or develop a central scar would also lead to increased ^{99m}Tc-MIBI uptake will require further investigation. Of note, the ^{99m}Tc-MIBI–avid oncocytoma reported by Gormley et al[9] was also quite large.

There may be multiple factors that play a role in the differential uptake of ^{99m}Tc-MIBI between oncocytomas and RCCs. First, as suggested previously, oncocytoma cells are packed with sheets of morphologically normal-appearing mitochondria.[7,8] Given the affinity of positively charged ^{99m}Tc-MIBI for the negative charge potential across the mitochondrial membrane, high uptake of ^{99m}Tc-MIBI in cells with a high mitochondrial load would be expected. In keeping with this, it is also noteworthy that RCCs have been demonstrated to contain decreased amounts of some mitochondrial proteins in comparison to the normal kidney,[15] which may reflect abnormal mitochondrial structure and function.

A second mechanism for the differential appearance of oncocytomas and RCC on ^{99m}Tc-MIBI imaging may be related to the presence of multidrug resistance (MDR) pumps on RCCs. These proteins are known to be highly expressed in RCC (notably in subtypes originating from the proximal tubule) as compared with oncocytoma,[16,17] which is a known mechanism for the elimination of MIBI from cells.[18] In fact, metastatic RCC have been noted to express high levels of MDR proteins to the extent that imaging ^{99m}Tc-MIBI uptake within a lesion can be used as a surrogate measure of the effectiveness of MDR blocking compounds that have been explored to improve the efficacy of cytotoxic chemotherapy.[10,11] Thus, it seems likely that the observed photopenia of the RCCs may at least partly derive from the active excretion of the radiotracer by the MDR proteins in their constituent cells.

Regardless of the exact mechanism underlying the significant difference in ^{99m}Tc-MIBI uptake between oncocytomas and RCCs, this finding could prove to be of great value in the future noninvasive evaluation of patients with solid enhancing renal masses. Given the inability of current anatomic imaging methods such as contrast-enhanced CT to reliably distinguish benign from malignant tumors, a definitive surgical

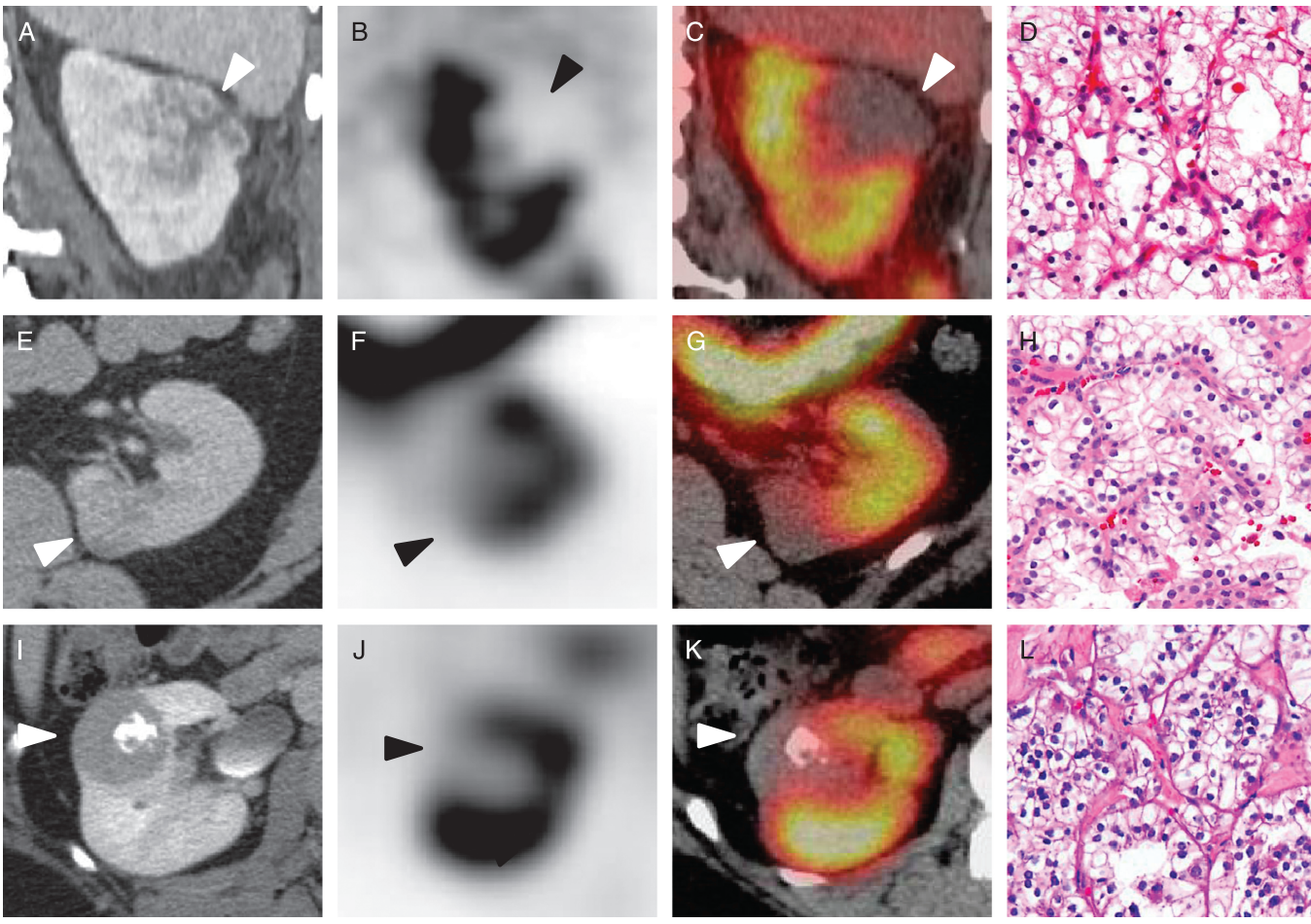

FIGURE 4. Representative images of the RCCs included in this study. **A**, Coronal contrast-enhanced CT, coronal SPECT (**B**), and coronal SPECT/CT fusion images of a left upper pole Fuhrman grade III clear cell RCC (**C**) with a representative histologic image (**D**, HE ×20) (patient 4, white and black arrowheads). **E**, Axial contrast-enhanced CT, axial SPECT (**F**), and axial SPECT/CT fusion images of a medial left lower pole unclassified RCC (**G**) with a corresponding histologic image (**H**, HE ×20) (patient 5, white and black arrowheads). **I**, Axial contrast-enhanced CT, axial SPECT (**J**), and axial SPECT/CT fusion images of an Xp11 translocation RCC (**K**) with a histologic image (**L**, HE ×20) (patient 6, white and black arrowheads).

pathology diagnosis is often required with a tacit acceptance that a measurable percentage of patients undergoing resection will have had an unnecessary major surgery. However, our results suggest that a simple imaging study with ^{99m}Tc-MIBI may be able to preoperatively identify those patients harboring an oncocytoma, thus sparing them from an unnecessary surgery.

Limitations of our study include the small sample size and the fact that we did not image all histologic variants of RCC. Of particular interest are the imaging characteristics of papillary and chromophobe RCC, both of which can contain varying amounts of oncocytic cells. To more rigorously assess the diagnostic accuracy of this imaging modality, we have initiated a clinical trial (ClinicalTrials.gov identifier NCT02160925) to prospectively study a large series of patients with clinical T1 renal tumors scheduled to undergo surgical resection. We expect to report the results of this trial by late 2015.

ACKNOWLEDGMENTS

The authors would like to thank Melvin J. Reinhardt, Danielle N. Rill, and Laura E. Grosse for the technical assistance.

REFERENCES

1. Gill IS, Aron M, Gervais DA, et al. Clinical practice. Small renal mass. *N Engl J Med*. 2010;362:624–634.
2. Hollingsworth JM, Miller DC, Daignault S, et al. Rising incidence of small renal masses: a need to reassess treatment effect. *J Natl Cancer Inst*. 2006;98:1331–1334.
3. Frank I, Blue ML, Cheville JC, et al. Solid renal tumors: an analysis of pathological features related to tumor size. *J Urol*. 2003;170:2217–2220.
4. Pierorazio PM, Hyams ES, Tsai S, et al. Multiphasic enhancement patterns of small renal masses (≤4 cm) on preoperative computed tomography: utility for distinguishing subtypes of renal cell carcinoma, angiomyolipoma, and oncoctyoma. *Urology*. 2013;81:1265–1271.
5. Pedrosa I, Sun MR, Spencer M, et al. MR imaging of renal masses: correlation with findings at surgery and pathologic analysis. *Radiographics*. 2008;28:985–1003.
6. Johnson DC, Vukina J, Smith AB, et al. Preoperatively misclassified, surgically removed benign renal masses: a systematic review of surgical series and United States population-level burden estimate. *J Urol*. 2015;193:30–35.
7. Krishnan B, Truong LD. Renal epithelial neoplasm: the diagnostic implications of electron microscropic study of 55 cases. *Hum Pathol*. 2002;33:68–79.
8. Johnson NB, Johnson MM, Seliq MK, et al. Use of electron microscopy in core biopsy diagnosis of oncocytic renal tumors. *Ultrastruct Pathol*. 2010;34:189–194.

9. Gormley TS, Van Every MJ, Moreno AJ. Renal oncocytoma: preoperative diagnosis using technetium 99m sestamibi imaging. *Urology*. 1996;48:33–39.
10. Williams KA, Hill KA, Sheridan CM. Noncardiac findings on dual-isotope myocardial perfusion SPECT. *J Nucl Cardiol*. 2003;10:395–402.
11. Derebek E, Kirkali Z, Dogan AS, et al. ^{99m}Tc-MIBI scintigraphy in metastatic renal cell carcinoma: clinical validation of the relationship between ^{99m}Tc-MIBI uptake and P-glycoprotein expression in tumor tissue. *Eur J Nucl Med*. 1996;23: 976–979.
12. Chen CC, Meadows B, Regis J, et al. Detection of in vivo P-glycoprotein inhibition by PSC 833 using Tc-99m sestamibi. *Clin Cancer Res*. 1997;3: 545–552.
13. Bates SE, Bakke S, Kang M, et al. A phase I/II study of infusional vinblastine with the P-glycoprotein antagonist valspodar (PSC 833) in renal cell carcinoma. *Clin Cancer Res*. 2004;10:4724–4733.
14. Hurwitz GA, Ghali SK, Mattar AG, et al. Dynamic renal imaging with technetium-99m-sestamibi in hypertension: potential for assessment of renovascular disorders. *J Nucl Med*. 1994;35:1959–1964.
15. Simonnet H, Alazard N, Pfeiffer K, et al. Low mitochondrial respiratory chain content correlates with tumor aggressiveness in renal cell carcinoma. *Carcinogensis*. 2002;23:759–768.
16. Rochlitz CF, Lobeck H, Peter S, et al. Multiple drug resistance gene expression in human renal cell cancer is associated with the histologic subtype. *Cancer*. 1992;15:2993–2998.
17. Tobe SW, Noble-Topham SE, Andrulis IL, et al. Expression of the multiple drug resistance gene in human renal cell carcinoma depends on tumor histology, grade, and stage. *Clin Cancer Res*. 1995;1:1611–1615.
18. Hendrikse NH, Franssen EJ, van der Graaf WT, et al. ^{99m}Tc-sestamibi is a substrate for P-glycoprotein and the multidrug resistance-associated protein. *Br J Cancer*. 1998;77:353–358.